Távérzékelt képsorozatok fúziós MRF szegmentálása

Fusion Markov Random Field Image Segmentation for a Time Series of Remote Sensed Images

Tamas Sziranyi, Andras Kriston, Tamas Csilling, Andras Majdik, Laszlo Tizedes

MTA SZTAKI, Budapest, Hungary
sziranyi;kriston;majdik;tizedes@sztaki.mta.hu

Abstract. Change detection on images of very different time instants from remote sensing databases and up-to-date satellite born or UAV born imaging is an emerging technology platform today. Since outdoor sceneries, principally observation of natural reserves, agricultural meadows and forest areas, are changing in illumination, coloring, textures and shadows time-by-time, and the resolution and geometrical properties of the imaging conditions may be also diverse, robust and semantic level algorithms should be developed for the comparison of images of the same or similar places in very different times. Earlier, a new method, fusion Markov Random Field (fMRF) method has been introduced which applied unsupervised or partly supervised clustering on a fused image series by using cross-layer similarity measure, followed by a multi-layer Markov Random Field segmentation. This paper shows the effective parametrization of the fusion MRF segmentation method for the analysis of agricultural areas of fine details and difficult subclasses.

1 Introduction[1]

As we have more and more remote sensing platforms for scanning the terrestrial surface, like satellite and airborne imaging, UAV based surveillance; and we have very different modalities as multi-band images, Lidar or Radar, the task to use them together in some fusion methodology and to find labelled changes among the very different scans needs new mathematical solutions. This paper presents a most recent methodology, where the different modalities of different time-instances can be fused to proceed a Markov Random Field (MRF) segmentation; the resulted label-map of fused MRF (fMRF [1]) is then used as master label-map to train the single layers for a forthcoming MRF segmentation procedure, where the single-layer MRF labeling can be compared to find labelled changes.

[1] Az ECMI'2018 konferencián megjelent "Segmentation and Change-Detection of Remote Sensing Images Using Fusion-MRF Model" c. cikk alapján (http://ecmi.bolyai.hu/upload/docs/ecmi_programguide.pdf)

The multi-band remote imaging methods, including UAV scanning from 20m - 100m altitudes, help us to collect data for agriculture/environmental protection analysis. When applying an appropriate energy optimization algorithm we can exploit labelled maps and we can track the changes through time and modalities. In precision farm management biomass monitoring is crucial. As shown in the study presented in [2] red, green and blue imaging obtained from UAV found to be a good alternative to other sensors used for precision agriculture. Dynamic monitoring of agricultural terraces in China was efficiently performed by the application of UAVs, [3]. The use of UAVs play a more and more significant role in monitoring natural hazards due to their cost efficiency and versatility, [4].

The main challenge is that the images of the series are very different in lighting, color and micro-structure. The framework of fMRF makes it possible to merge different data-structures, even for semi-supervised parameter-setting, like in [5] for Lidar ground-truths.

In our tests we used 3DR Solo[2] UAV for data capturing, equipped with an RGB and a four channel (Green-550 nm, Red-660 nm, Red edge -735 nm, Near infrared -790 nm) multispectral camera system (i.e. Parrot Sequoia) over the farming site in the vicinity of Biatorbagy town, Budapest metropolitan area, Hungary. In the course of the multi-session mapping we captured more than 2,100 narrow-band 1.2 mega pixel images covering 8 hectare (ha) of fruit and vineyard. Next, geo-referenced orthomosaic photo was computed corresponding to every multispectral band captured at different time instances using the Pix4D[3] software tools.

2 Fusion MRF

Fusion MRF (fMRF) has been introduced in [1] for remote sensing change detection. Different multilayer MRF based algorithms have been compared for change detection in [6], where fMRF proved to be most effective in some change detection tasks, as Fig. 1 shows. This fusion based method has been also used in a recent project, where aerial Lidar and satellite born images have been fused in a new MRF based solution to find small wetland areas [5].

In a series of N layers of remote sensing images, let $\overline{x}_s^{L_i}$ denote the feature vector at pixel s of layer L_i, $i = 1, 2, \cdots, N$. This feature vector might contain color, texture/micro-structural features, cross layer similarity measures, or mixture of these. Set $X = \{\overline{x}_s | s \in S\}$ marks the global image data. An example of a feature vector would be

$$\overline{x}_s^{L_i} = [\overline{x}_{C(s)}^{L_i}, \overline{x}_{M(s)}^{L_i}]^T \tag{1}$$

where $\overline{x}_{C(s)}^{L_i}$ contains the pixel's color values, and $\overline{x}_{M(s)}^{L_i}$ is the cross layer similarity measures between the image and other two or more images in the series. The cross layer similarity measure might be correlation, mutual information, or

[2] 3DR Solo: https://3dr.com/solo-drone/
[3] Pix4d photogrammetry software: https://pix4d.com

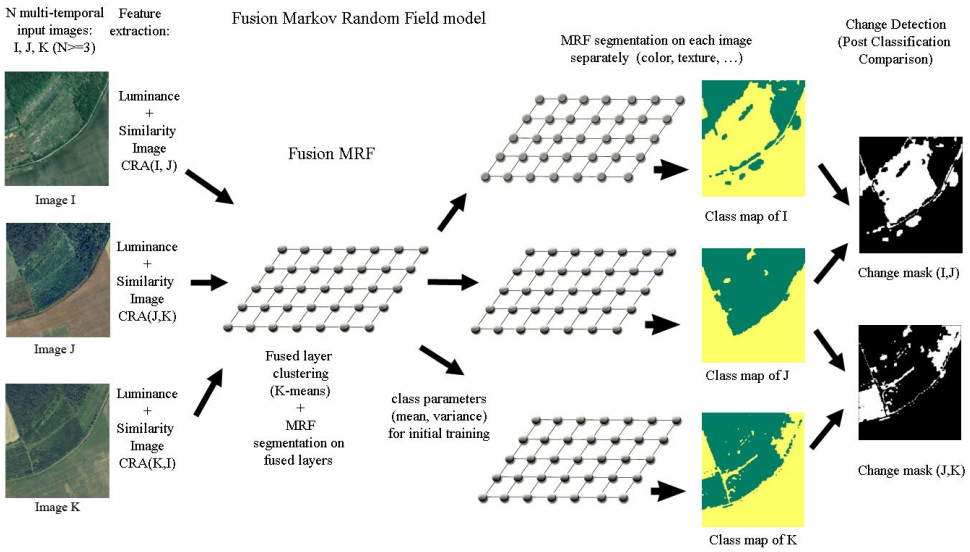

Fig. 1. The model of fusion MRF in case of 3 different time instants of scanning (Luminance-CRA feature-set) [1][6]

CRA. In this study Cluster Reward Algorithm (CRA) was used [7], defined between image pairs, calculated using the joint histogram of the two images and the marginal histograms, see more in [1].

The multiple layers of remote sensed image time series are characterized by the stack $\overline{x}_s^{L_{i_1 \dots i_n}}$ of these vectors for a reasonable set of them, $n \leq N$:

$$\overline{x}_s^{L_{i_1 \dots i_n}} = \{\overline{x}_s^{L_{i_1}}, \overline{x}_s^{L_{i_2}}, \dots \overline{x}_s^{L_{i_n}}\} \tag{2}$$

2.1 Fusion-MRF: multi-layer segmentation and change detection

For MRF segmentation, more details can be found in [8], [9], [10], [11]. Once feature vectors are generated, the six steps of the algorithm proposed here are applied, as it is introduced in [1]. This segmentation and change detection procedure contains different levels of MRF optimization in the following main steps:

1. Selecting and registering the image layers; In case of professional data suppliers orthonormed and geographically registered images are given; no further registration is needed. In our method no color-constancy or any shape/color semantic information is needed; the color of the corresponding areas and the texture can differ strongly layer-by-layer.
2. Finding clusters in the set of vectors ($\overline{x}_s^{L_{i_1 \dots i_n}}$) and calculating the cluster parameters (mean and covariance) for the fusion based "*multi-layer clusters*". This step can be performed by using unsupervised methods such as the K-means algorithm.

3. Running MRF segmentation on the fused layer data ($\overline{x}_s^{L_{i_1 \dots i_n}}$) containing the cross-layer measures (refer to similarity measure in [1]), and the multi-layer cluster parameters, resulting in a multi-layer labeling $\Omega_{L_{i_1 \dots i_n}}$;
4. Single-layer training: the map of multi-layer labeling $\Omega_{L_{i_1 \dots i_n}}$ is used as a training map for each image layer L_i: cluster parameters are calculated for each single layer controlled by the label map of multi-layer clusters.
5. For each label $k \in \Lambda$ the corresponding subspace of ($\overline{x}_s^{ML_n}$) are collected;
6. For each single layer L_i (containing only its color and maybe texture features) a MRF segmentation is processed, resulting in a labeling: Ω_{L_i};
7. The consecutive image layers $(..., (i-1), (i), ...)$ are compared to find the changes among the different label maps to get the change map.

The above fusion MRF model and its processing can be seen in Fig. 1, [1][6]. In our application a graph cut based α-expansion algorithm was used for energy minimization of MRF, with the adherent implementation of [10].

3 Segmentation of UAV based remote sensed image time series

During the measurement series, data was collected from April, June and July. The vegetation - thus the difference between images - is expected to change quite much between April and June and less between June and July. The vegetation intensity, health of plants, soil composition, presence of water or building can be analyzed by the near infrared band of the image. Since living plants with more chlorophyll reflect more near-infrared energy they appear darker on the images which makes their classification more accurate. Non-supervised segmentation is performed to see the evolution of vegetation from one month to the other and to observe locations where changes occur.

In this study the red, green and red-edge bands were used to create the feature vectors for the fMRF model and two different feature-sets were tested. In the *multi-band feature-set* a twelve element vector was created for each pixel of the three image stack: red - green - red-edge values, Normalized Difference Vegetation Index (NDVI); NDVI = (red-edge - red) / (red-edge + red);

Fig. 2 shows results of FMRF segmentation using only spectral channels and only similarity measure as feature-set. The images were classified into four classes which would represent the bare soil, low and high vegetation plant covered areas and the roads covered by rocks or buildings. The comparison of labeled regions and corresponding original RGB areas is shown by Fig. 3. Rectangles 1,2,3 and 4 indicate the classes which were separated by the segmentation process. Dark blue color was given to bare soil,light blue to roads and buildings, green to high intensity vegetation and red to low intensity vegetation, respectively.

In the case of both processing steps (fused layer clustering and MRF; single layer MRF) the above detailed feature vectors were applied. This feature setting is powerful when there are image layers with color variation of nearly obvious clusters.

Fig. 4 shows the original input images from 3 consecutive months, then the fused master fMRF images originated from the inputs for different CRA window sizes. We see that the level of details can be tuned by the CRA window, characteristic for the microstructure similarity.

Based on the master fMRF label-maps, segmentation for each single layer can be proceeded, getting unified labelling to all the layer. Fig. 7 shows a segmentation result on the left, with a GroundTruth label-map on the right. The label-mapping Recall error evaluation can be found in Table 1.

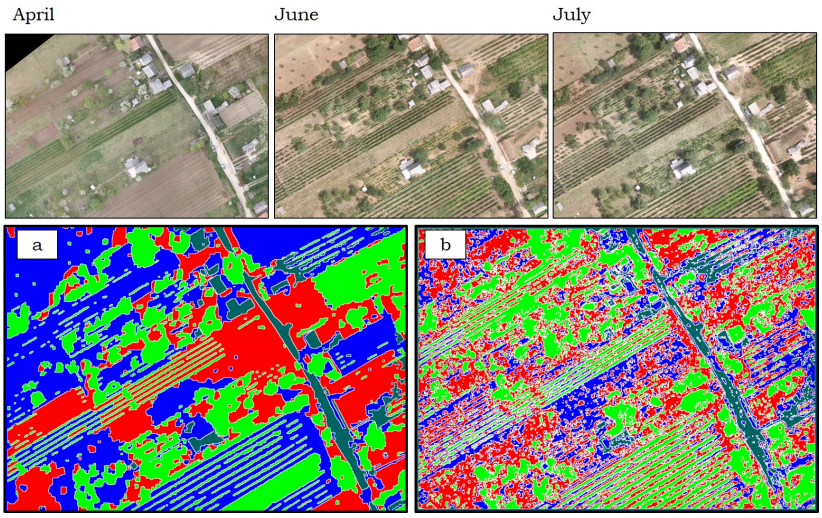

Fig. 2. Original images used for creating fused layer by K–means clustering and MRF segmentation. a) is the result of using the spectral channels, while b) is the result of using only similarity measure for segmentation.

Table 1. Recall values for the segmentation results, for the image taken in July.

Class	*4-channel multi-band set*	*Luminance + CRA statistical measure*
High Intensity Vegetation	0.84	0.52
Low Intensity Vegetation	0.26	0.62
Buildings/Roads	0.82	0.8
Bare Soil	0.67	0.16

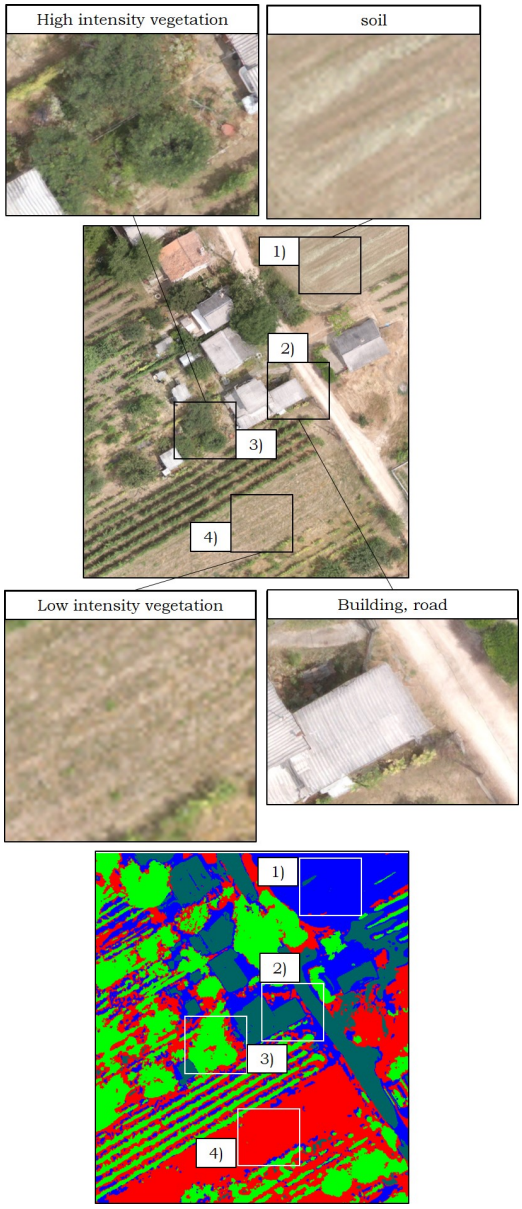

Fig. 3. Classes of agricultural image. The following classes are expected to be separated in the final segmentation: bare soil, roads or buildings, high intensity vegetation and low intensity vegetation.

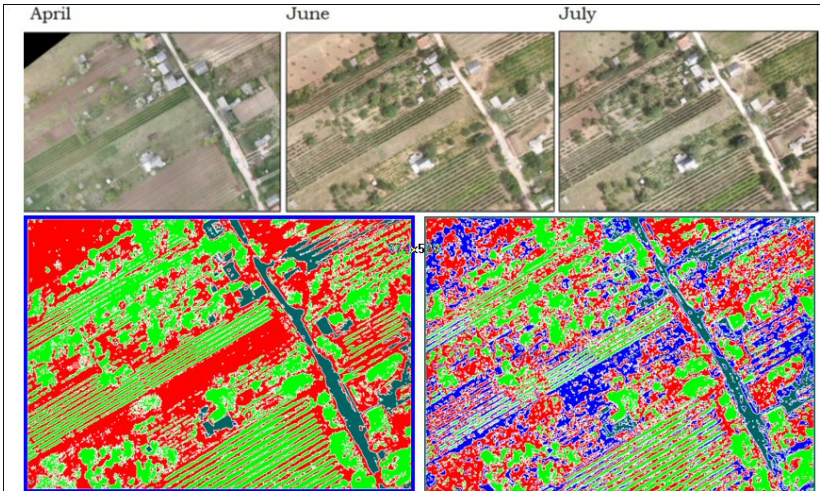

Fig. 4. Original images used for creating fused layer by K–means clustering and fMRF segmentation based on 4 color channels and CRA fine-texture statistical distance: above is the series of 3 input images of different time instants, while below the fused master-maps: left with CRA windows of 15, right with CRA windows of 7. Clusters are: meadows, vinegard, trees, road, house.

4 Change Detection and its Interpretation

The changed areas were simply determined by comparing the segmented images to each other, and mark where pixel label differs on the two images, see Fig. 9 . The changed areas were marked with white, while unchanged areas with black. The results are presented in two columns for each pair (April-June and June-July) in order to compare the effects of the two feature-sets. Rectangle-1 and Rectangle-2 highlight representative areas where the change detection is investigated. The area surrounded by Rectangle-1 includes grassland, road, building and vines as well. Yellow arrow points to the grassland areas, while blue shows the location of a building. The Rectangle-2 crops a field containing vines, grassland and trees. On this region, purple arrow points to grassland, while red arrows mark an area with vines and trees. The change detection for building within Rectangle-1 should not indicate any alteration since its composition and location is unchanged during the time period. The only thing which could affect its appearance is the lighting condition.

The following observation were taken: April-June, feature-set 1) - In the Rectangle-1, a triangle shaped grassland field was classified with the same label for both moths, except a small part. Thus, algorithm says there was no change (black), only a little one (white). feature-set 2) result is inverse to the first one; here this particular field seems totally changed. The house (pointed by blue arrow) mostly looks unchanged with feature-set 1), as expected, but entirely changed by feature-set 2) which is wrong. In the Rectangle-2, grassland pointed by purple arrow, looks partially change by feature-set 1) while almost unchanged

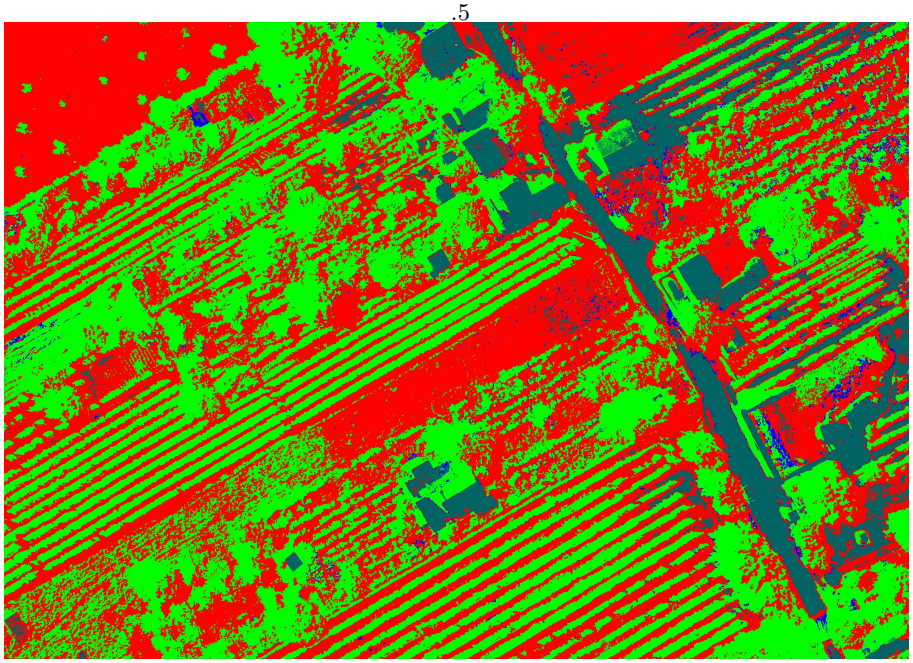

Fig. 5. Single layer segmentation

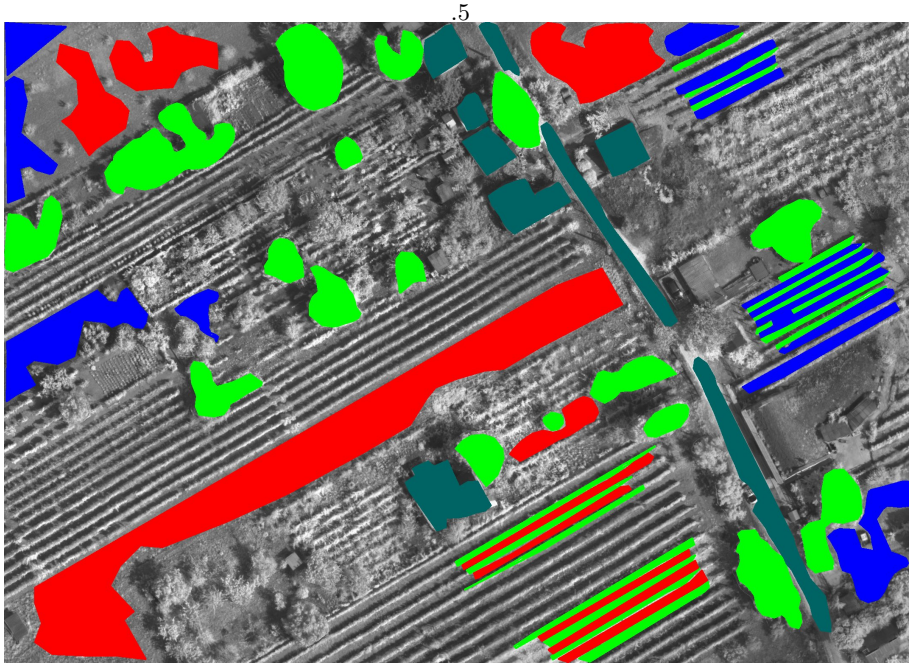

Fig. 6. GroundTruth reference label-map

Fig. 7. Single layer mapping; left: Segmented single layer of July, trained by the label-map of fMRF master (CRA width: 15); right: GoundTruth label-map for comparison

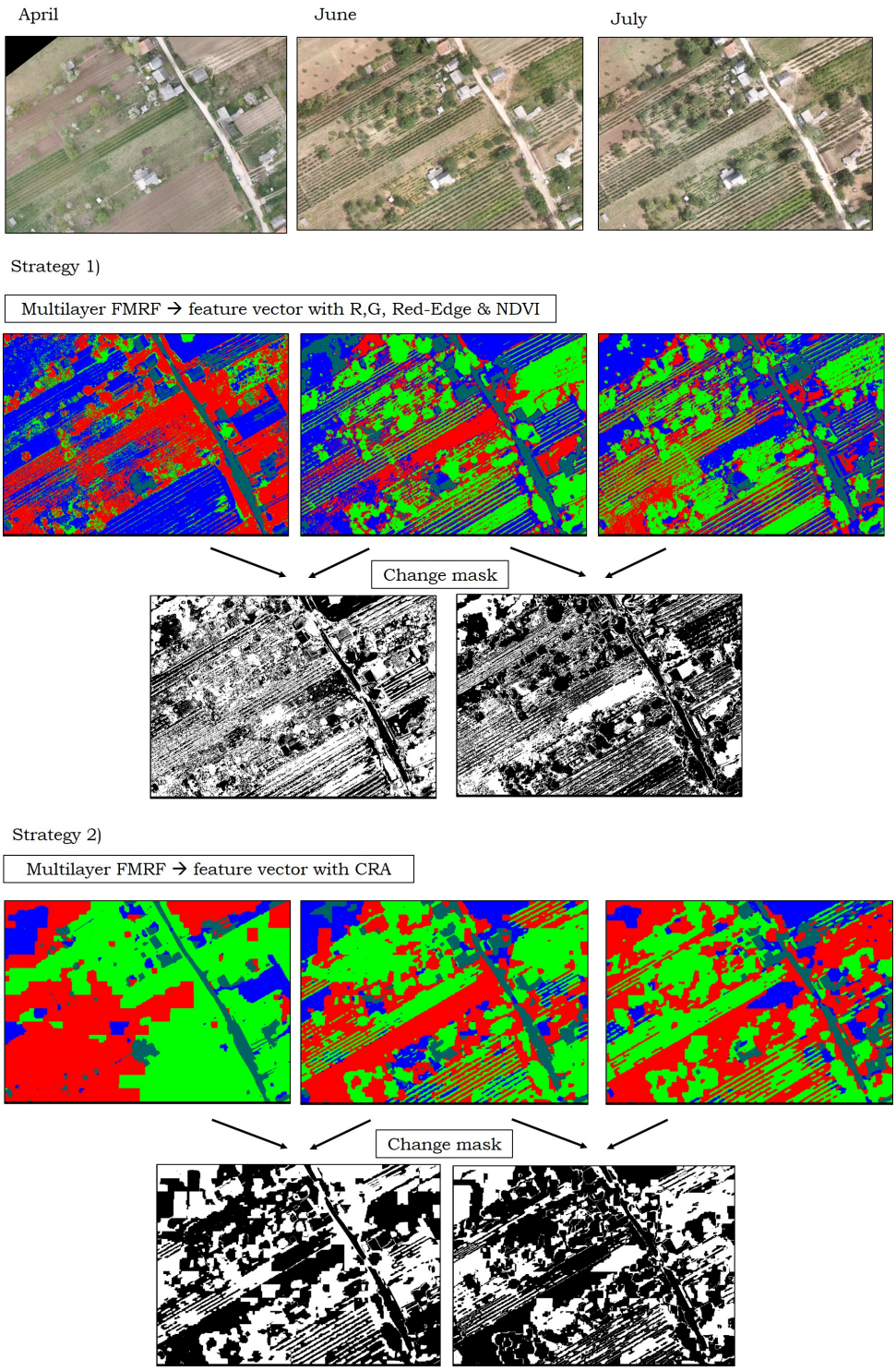

Fig. 8. Representative RGB images and the segmentation results of the two feature-sets. The colors correspond the the following classes: dark blue - bare soil, light blue - rock covered roads and buildings, green - high intensity vegetation area, red - low intensity vegetation area. Black and white images are change maps, where white show regions that changed during time and black indicates unchanged areas.

by feature-set 2). In the area marked by the red arrow, vines become more visible due to the new leaves, thus change occur as it was indicated by feature-set 1). A tree, just at the tip of the red arrow, appear on the image taken in June, which is not noticeable in April (dashed circle shows its location). Both feature-sets correctly marked this pixel area with white since change occurred. June-July, feature-set 1) - In Rectangle-1, one can now detect some changes. The field looks like bare soil in June but more like grassland in July. It is also noticeable that the paths left by a machinery which cut the grass, show some changes (yellow arrow). As well as one can see a straw in the image taken in July marked with a dashed line circle. House (pointed by blue arrow) seems to be mostly unchanged. On the change map created by feature-set 2) this grassland field seems unchanged. The newly grown grass did not cause any changes in the segmentation process. In the Rectangle-2, grassland field indicated by purple arrow is marked as changed areas with feature-set 1) but not with feature-set 2). The tree visible on both images is correctly marked as unchanged region by both feature-set. The black and white lines in the change map of feature-set 1) show the growing vines (white) and the unchanged condition in the soil. Overall one see that as it was expected more changes occurred from April to June, and less from June to July. The following changes were determined given in percentage over the months. In the case of feature-set 1); from April to June 56%, from June to July 42% and from April to July 60% changes occurred the images. In the case of feature-set 2); from April to June 46%, from June to July 40% and from April to July 54% changes occurred.

5 Conclusion

Unsupervised clustering on multilayer image dataset combined with MRF segmentation is a powerful tool to segment multispectral images into relevant classes. When MRF segmentation is used for multi-band+CRA images we may get proper results. In case of severe combination of subclasses due to heavy differences in lighting and color content, the fused MRF segmentation is better to use fine-structure information, as the CRA.

References

1. Sziranyi, T., Shadaydeh, M.: Segmentation of remote sensing images using similarity-measure-based fusion-mrf model. IEEE Geoscience and Remote Sensing Letters **11** (2014) 1544–1548
2. Ballesteros, R., Ortega, J.F., Hernandez, D., Moreno, M.A.: Onion biomass monitoring using uavbased rgb imaging. Precision Agriculture (2018)
3. Wei, Z., Han, Y., Li, M., Yang, K., Yang, Y., Luo, Y., Ong, S.H.: A small UAV based multi-temporal image registration for dynamic agricultural terrace monitoring. Remote Sensing **9** (2017) 904
4. Giordan, D., Manconib, A., Remondinoc, F., Nexd, F.: Use of unmanned aerial vehicles in monitoring application and management of natural hazards. Geomatics, Natural Hazards and Risk **8** (2017) 1–4

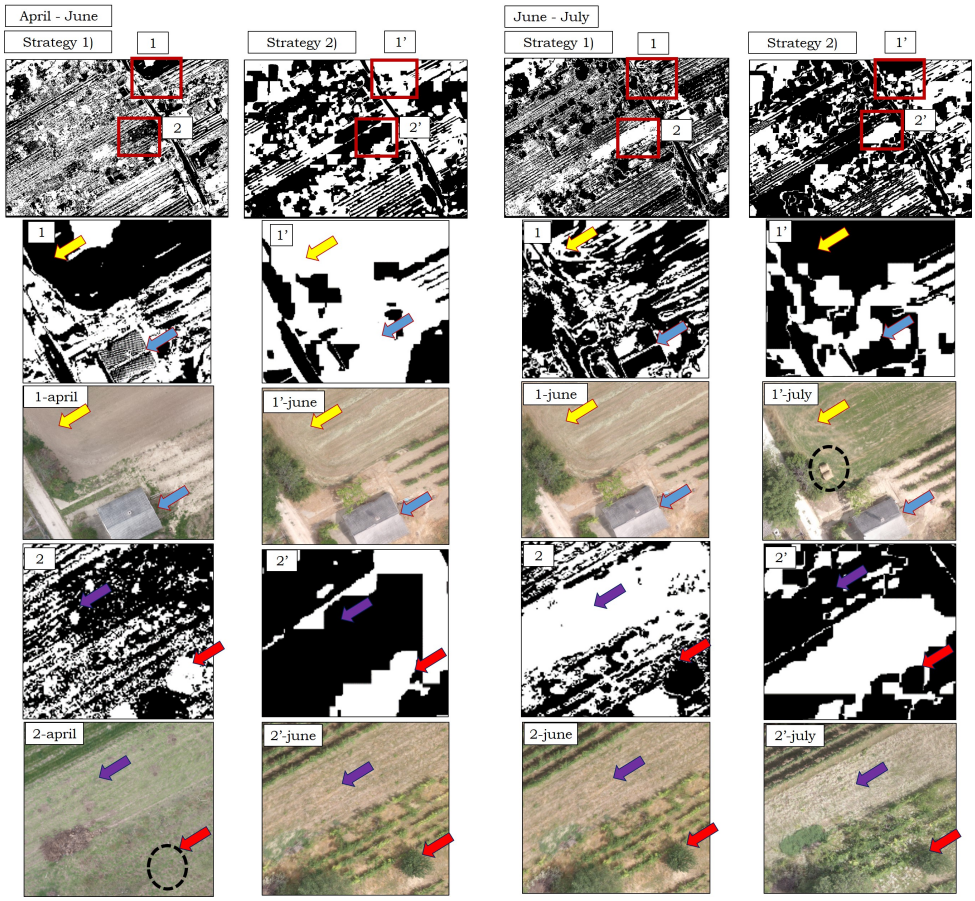

Fig. 9. Resulted change maps with the two different feature-sets. White shows changes while black shows unchanged areas. Rectangles 1, 1' and 2, 2' show representative areas of two feature-sets. Arrows point to locations where resulted change detection is under investigation.Yellow, and purple arrows point to grassland, blue points to a building and red indicates an area where trees and vines can be seen.

5. Shadaydeh, M., Zlinszky, A., Manno-Kovacs, A., Sziranyi, T.: Wetland mapping by fusion of airborne laser scanning and multi-temporal multispectral satellite imagery. International Journal of Remote Sensing **38** (2017) 7422–7440
6. Benedek, C., Shadaydeh, M., Kato, Z., Sziranyi, T., Zerubia, J.: Multilayer markov random field models for change detection in optical remote sensing images. ISPRS Journal of Photogrammetry and Remote Sensing **107** (2015) 22 – 37 Multitemporal remote sensing data analysis.
7. Inglada, J., Giros, A.: On the possibility of automatic multisensor image registration. IEEE Trans. Geosci. and Remote Sensing **42** (2004) 2104–2120
8. Benedek, C., Sziranyi, T.: Change detection in optical aerial images by a multilayer conditional mixed Markov model. IEEE Trans. Geosci. and Remote Sensing **47** (2009) 3416–3430
9. Geman, S., Geman, D.: Stochastic relaxation, Gibbs distributions and the Bayesian restoration of images. IEEE Trans. Pattern Analysis and Machine Intelligence (1984) 721–741
10. Szeliski, R., Zabih, R., Scharstein, D., Veksler, O., Kolmogorov, V., Agarwala, A., Tappen, M., Rother, C.: A comparative study of energy minimization methods for Markov Random Fields. In: 9th ECCV. Volume 2. (2006) 16–29
11. Kato, Z., Zerubia, J., Berthod, M.: Unsupervised parallel image classification using Markovian models. Pattern Recognition **32** (1999) 591–604